

Resultant pressure distribution pattern along the basilar membrane in the spiral shaped cochlea

Yong Zhang* and Chul Koo Kim[†]

Institute of Physics and Applied Physics,

Yonsei University, Seoul 120-749, Korea

Kong-Ju-Bock Lee[‡]

Department of Physics, Ewha Womans University, Seoul 120-750, Korea and

School of Physics, Korea Institute for Advanced Study, Seoul 130-722, Korea

Youngah Park[§]

Department of Physics, Myongji University, Yongin 449-728, Korea and

School of Physics, Korea Institute for Advanced Study, Seoul 130-722, Korea

Abstract

Cochlea is an important auditory organ in the inner ear. In most mammals, it is coiled as a spiral. Whether this specific shape influences hearing is still an open problem. By employing a three dimensional fluid model of the cochlea with an idealized geometry, the influence of the spiral geometry of the cochlea is examined. We obtain solutions of the model through a conformal transformation in a long-wave approximation. Our results show that the net pressure acting on the basilar membrane is not uniform along its spanwise direction. Also, it is shown that the location of the maximum of the spanwise pressure difference in the axial direction has a mode dependence. In the simplest pattern, the present result is consistent with the previous theory based on the WKB-like approximation [D. Manoussaki, *et al.*, Phys. Rev. Lett. **96**, 088701 (2006)]. In this mode, the pressure difference in the spanwise direction is a monotonic function of the distance from the apex and the normal velocity across the channel width is zero. Thus in the lowest order approximation, we can neglect the existence of the Reissner's membrane in the upper channel. However, higher responsive modes show different behavior and, thus, the real maximum is expected to be located not exactly at the apex, but at a position determined by the spiral geometry of the cochlea and the width of the cochlear duct. In these modes, the spanwise normal velocities are not zero. Thus, it indicates that one should take into account of the detailed geometry of the cochlear duct for a more quantitative result. The present result clearly demonstrates that not only the spiral geometry, but also the geometry of the cochlear duct play decisive roles in distributing the wave energy.

PACS numbers: 43.64.Kc,43.64.Ri

*Electronic address: xyzhang@phya.yonsei.ac.kr

†Electronic address: ckkim@yonsei.ac.kr

‡Electronic address: kjblee@ewha.ac.kr

§Electronic address: youngah@mju.ac.kr

I. INTRODUCTION

The primary functions of the mammalian cochlea are to detect and analyze the acoustic signals in terms of their intensity and frequency contents. It is able to probe and analyze sound waves over wide ranges of frequency and intensity, e.g., for human being, over twelve orders in intensity and over three orders in frequency (20Hz – 20kHz) [1]. Some mammals are able to perceive frequencies as high as 100kHz [2]. Remarkable capabilities appearing in hearing are essentially governed by both passive mechanical and active biophysical procedures in the cochlea. The physics of hearing is pioneered by von Helmholtz in 1880s [3]. He proposed that different regions along the longitudinal length of the cochlea vibrate independently, working as a series of oscillators driven by the pressure of the fluid filled in the cavity of the cochlea. The coupling among the successive parts of the cochlea is thought to be mainly determined through the fluid, instead of the cochlea itself. Benefitted from the achievements in both the experimental techniques and the theoretical methods, auditory physics has been developing continuously from the time of von Helmholtz and expanding on ever-widening problems [2, 4, 5, 6].

Observations revealed that the cochleae are coiled in almost all mammals, monotremes being the exceptions. This auditory apparatus is a fully fluid-filled system of canals contained inside the petrous bone. It suggests that detailed calculation of the fluid motion and the pressure distribution within the cochlea should be crucial for understanding of hearing in any mechanical models of the cochlea. Fluid in the cochlea is a lymph. Physically, it can be treated as incompressible and inviscid as a reasonable approximation [7]. The cavity of the cochlea is partitioned by the basilar membrane (BM) into two channels which are connected through the helicotrema at the apex of the cochlea. At the other end, the base, the channels are sealed by two movable membranes working as pistons. These two movable membranes are labeled as the oval and the round windows, respectively. The channel abutting to the oval window is named as scala vestibuli (upper channel). Another channel abutting to the round window is known as scala tympani (lower channel). The upper channel is further separated by the Reissner's membrane (RM) into two subducts. However, the RM is usually ignored in the mechanical models for the cochlea because of its extreme flexibility, when the axial flow behavior is the main focus. As a consequence, the structure of the cochlea is typically modeled by two channels with the BM as their interface in most mechanical

studies. However, when the spanwise pressure distribution is included in the study, the RM affects the flow characteristics and, thus, cannot be neglected. We will address this problem below.

The stapes is attached on the oval window and forms the boundary between the middle and the inner ear. Incoming sound waves are transmitted into the fluid in the channels of the cochlea through the vibration of the stapes. Nearly entire mechanical sound energy exerted by the stapes is used to produce the fluid movement. The sound pressure transmitted to the cochlear fluid interacts mechanically with the BM and vibrates it into oscillation in the form of a traveling wave that propagates along the BM from the base to the apex. The traveling wave on the BM grows as it travels, reaching a maximum at a position known as the characteristic place determined by the frequency of the stimulus, and then declines rapidly. The characteristic behavior along the longitudinal cochlea is described by a place-frequency map; high frequencies are resonant near the basal end, whereas low frequencies are resonant near the apical end [4].

The first direct observation of the responses of the BM to sounds through experiment was achieved by von Békésy [8]. He measured the BM movement of the cadaver and found that the mechanical response is a traveling wave propagating from the base to the apex. Subsequent in-vivo measurements revealed that the responses of the BM are sharply tuned and very sensitive at low sound-pressure levels. Hence it is evident that hearing involves an active process. However, a passive mechanism also plays an essential role in hearing and also in understanding the auditory phenomena.

Although the spiral coiling is one of the most distinct characters of the cochlea, it has been neglected in many mechanical models [5]. Therefore, it is one of the prime interests to ask whether the shape of the cochlea influences hearing or just facilitates the packing of the long BM into a small space. If the answer is the latter, then the cochlea can be safely modeled as a straightly shaped duct to avoid the complexity of the spiral shape. Due to the mathematical difficulties in dealing with the shape of the cochlea, this problem has not been fully answered yet. Earlier studies mostly concluded that the shape of the cochlea has little effect on the response of the BM along the center line [8, 9, 10, 11]. However, recently, Manoussaki *et. al.* employed a WKB-like and linearly approximated solution to examine the effect of the curvature of the cochlea on the redistribution of the wave energy density. According to their linear expansion, it was concluded that the spiral geometry of the cochlea

does play an essential role in creating a tilt of the BM between the outer and the inner wall, which is believed to be important to produce the vibration of the hair cells. The calculated tilt is shown to be proportional to the curvature of the center line of the cochlea and, thus, the maximum of the tilt is predicted to be always at the apex [12]. In the present paper, we employ a three dimensional fluid model without the assumption of the WKB-like solution. By employing a conformal transformation and a long-wave approximation, we explicitly obtain the solutions of the fluid model which satisfies the boundary condition.

Our analytic solution shows that the Manoussaki *et al*'s solution [12] is naturally included as the lowest component of the general solutions, and has no flux across the channel width. The general solution shows that the resultant pressure acting on the BM is not uniform across the channel width. It is shown that different responsive modes show different patterns of the spanwise pressure tilt along the longitudinal length of the BM. Especially, for higher modes which allow the flux across the channel width, the magnitude of the pressure tilt is not always a monotonic function of the curvature as predicted by Manoussaki *et al.* [12]. Since the real fluid oscillation is a linear superposition of several modes, we expect that the the maximum of the resultant pressure tilt is not located exactly at the apex as predicted by Manoussaki *et al.* [12], but at a position determined by the input wave and the geometry of the cochlea.

The arrangement of this paper is as follows. In Sec. II, we give the fluid model of the cochlea and calculate the velocity potential and the flow of the fluid in the duct of the cochlea. Sec. III discusses the pressure in the fluid using the Navier-Stokes equation. Sec. IV gives a discussion on the results. Sec. V concludes the paper.

II. MECHANICAL MODEL

Because most mammalian cochleae are coiled into a spiral, the cochlea is approximately modeled as a logarithmic spiral duct with a rectangular cross section and the RM is approximately considered as the center line in the upper channel as shown in Fig. 1, although the detailed geometry is much more complicated. We also assume that it stays in plane in the present model although the center line of the cochlea coils out-of-plane in reality, The BM partitions the duct into two channels, the upper and the lower channels. The height and the width of the cochlea are assumed uniform along its longitudinal length. In what follows,

we mainly discuss the response of the fluid in the outer part of the upper channel, between the RM and the outer wall using our idealized geometry. The result can be extended to the lower channel by considering the connectivity of the helicotrema and the symmetry as elaborated in the references [12, 13]. Cochlea fluid is approximated as incompressible and irrotational, i.e., $\nabla \cdot \mathbf{U} = 0$ and $\nabla \times \mathbf{U} = 0$, where \mathbf{U} is the velocity of the fluid. Hence the velocity of the fluid in the cochlea can be described in terms of the velocity potential, $\mathbf{U} = \nabla\Phi$. Thus, the velocity potential Φ satisfies the Laplace equation

$$\nabla^2\Phi = 0. \quad (1)$$

In the cylindrical polar coordinate system,

$$\nabla^2 = \frac{\partial^2}{\partial R^2} + \frac{1}{R} \frac{\partial}{\partial R} + \frac{1}{R^2} \frac{\partial^2}{\partial \Theta^2} + \frac{\partial^2}{\partial \zeta^2}, \quad (2)$$

where R and Θ are the coordinates in the plane of the BM; ζ is the coordinate perpendicular to the BM. At the apex, the polar angle is zero and at the spiral axis, $R = 0$. Recently Manoussaki *et al.* studied the cochlea curvature effect on the radial shearing in the BM region [12]. Instead of solving the Laplace equation, Eq. (1) directly, they assumed a WKB-like propagating wave solution,

$$\Phi = \Phi_0(R, \Theta, \zeta) \exp \left[i\omega t - i \int_0^\Theta K(\Theta) R_m(\Theta) d\Theta \right], \quad (3)$$

where Φ_0 is a slowly varying function of the angular coordinate Θ , R_m the distance to the spiral duct midline from the spiral axis, K the axial wave number, and ω the input frequency. They applied this solution to the continuity and interface equations of the BM motion to obtain the BM displacement. In the first order approximation, they found that the displacement of the BM-fluid interface gets tilted across the width of the partition and the spanwise amplitude slope varies as $1/R_m$. Thus, they predicted that the maximum of the tilt to be always at the apex in the long-wavelength limit and the spiral shape of the cochlea plays an important role in distributing the wave energy density towards the cochlea's outer wall.

However, it is believed that the pressure is transmitted through the fluid and not through the BM itself. Therefore, it is necessary to study the detailed fluid response to the applied pressure in order to obtain detailed information on the pressure redistribution and the sound propagation. In the present study, we solve the Laplace equation directly without the

assumption of the WKB-like plane wave solution. Since the above equation does not contain any explicit time-dependence, solutions of this equation cannot describe propagation of the waves along the cochlea. However, it can give information on the spanwise distribution of the pressure on the BM of the steady response. It has been demonstrated that at least to the first order approximation, the in-phase assumption is a good approximation to discuss the spanwise profile of the BM [14]. Separating the variable, ζ , from the rest two variables, we have $\Phi(R, \Theta, \zeta, t) = \phi(R, \Theta)H(\zeta)T(t)$. Eq. (1) is separated into two independent parts

$$\frac{\partial^2 H(\zeta)}{\partial \zeta^2} = \mu^2 H(\zeta), \quad (4)$$

$$\frac{\partial^2 \phi}{\partial R^2} + \frac{1}{R} \frac{\partial \phi}{\partial R} + \frac{1}{R^2} \frac{\partial^2 \phi}{\partial \Theta^2} = -\mu^2 \phi, \quad (5)$$

where μ is a separation constant that can be any constant. Here, we note that if we apply the WKB-like solution, Eq. (3), to Eq. (5), we obtain the same result as in Ref. [12]. Now, we impose a boundary condition that the wall of the cochlea is impermeable, i.e., the velocity of the fluid normal to the wall is zero on the walls of the cochlea. However, because the RM is extremely flexible, the velocity normal to the RM is not necessarily zero. Since the RM is fixed on the BM, the pressure distribution near the intersection line between the RM and the BM is expected to be much complicated. The solution for such a case can only be obtained through very complicated numerical calculations. Since, it is the aim of this paper to investigate the curvature effect of the cochlea and improve from the WKB-like solution, we neglect the edge effect and assume that the RM behaves as a free boundary. Therefore, the solution of the velocity potential in the vertical direction to the BM is

$$H(\zeta) = \cosh [\mu(\zeta - h)], \quad (6)$$

where h is the half height of the cochlea. For simplicity, we assume that μ is sufficiently small, $\mu \ll 1$. Note that the small μ corresponds to a long-wave approximation [12, 15]. We will discuss later that the small μ is also related to a weak stimulation. Accordingly, Eq. (5) is approximately rewritten as

$$\frac{\partial^2 \phi}{\partial R^2} + \frac{1}{R} \frac{\partial \phi}{\partial R} + \frac{1}{R^2} \frac{\partial^2 \phi}{\partial \Theta^2} = 0. \quad (7)$$

The solution of Eq. (7) thus can be obtained as

$$\phi(R, \Theta) = (A_l \cos l\Theta + B_l \sin l\Theta)R^l, \quad (8)$$

where l is any integer and $A_l(B_l)$ the constants to be determined by the boundary conditions. R^{-l} terms are neglected to avoid diverging contributions at small R . In order to employ techniques developed in the harmonic functions, the velocity potential, ϕ , is rewritten in a complex plane

$$\phi = [A_l(z^l + \bar{z}^l) - iB_l(z^l - \bar{z}^l)], \quad (9)$$

where $z = R \exp(i\Theta)$ and \bar{z} is the complex conjugate of z . The solution should satisfy the boundary condition, impermeability of the spiral walls. It thus requires to recombine these separated variables together in an appropriate way, so that the spiral boundary condition can be conveniently achieved. Conformal transformation is a natural way to achieve it. We introduce a complex potential, $f = \phi + i\varphi$. For f being analytic, ϕ and φ must satisfy the Riemann-Cauchy relation,

$$\frac{\partial \phi}{\partial x} = \frac{\partial \varphi}{\partial y}, \quad \frac{\partial \phi}{\partial y} = -\frac{\partial \varphi}{\partial x}, \quad (10)$$

where x and y are the real and the imaginary parts of the complex variable, z , i.e., $z = x + iy$. It is easy to verify that the imaginary part of the complex potential is the streamline of the fluid, $\varphi = -[A_l(z^l + \bar{z}^l) + iB_l(z^l - \bar{z}^l)]$. The complex potential is thus

$$f = z^l [A_l - iB_l]. \quad (11)$$

Now, we introduce a conformal transformation

$$w = \rho_o e^{-iz}, \quad (12)$$

where ρ_o is chosen to be the distance from the origin of the spiral axis to the outer wall of the apex. After the conformal transformation, the complex potential has the form

$$f = \left(i \ln \frac{w}{\rho_o} \right)^l (A_l - iB_l). \quad (13)$$

Using that $w = r \exp[i\theta]$ in the polar representation,

$$f = \left[-\theta + i \ln \frac{r}{\rho_o} \right]^l (A_l - iB_l). \quad (14)$$

The horizontal velocity potential $\phi(r, \theta)$ is the real part of the complex potential [16]. Combining the horizontal and the vertical parts of the velocity potential, one has

$$\Phi(r, \theta, \zeta, t) = \phi(r, \theta) H(\zeta) T(t) = \text{Re}(f) H(\zeta) T(t), \quad (15)$$

where $Re(f)$ is the real part of the complex potential f . Accordingly, the velocity potential is also a function of l . Different l corresponds to each different responsive mode. To distinguish different modes, we introduce a suffix l into the two-dimensional and the three dimensional velocity potential, velocity and pressure, i.e., ϕ_l , Φ_l , U_l and P_l , respectively. In general,

$$\begin{aligned} \phi_l(r, \theta) = & A_l \sum_{n=0}^{\lfloor l/2 \rfloor} (-1)^{l-n} \binom{l}{2n} \left(\ln \frac{r}{\rho_o} \right)^{2n} \theta^{l-2n} \\ & + B_l \sum_{m=1}^{\lfloor (l+1)/2 \rfloor} (-1)^{l-m} \binom{l}{2m-1} \left(\ln \frac{r}{\rho_o} \right)^{2m-1} \theta^{l-2m+1}, \end{aligned} \quad (16)$$

where $\lfloor x \rfloor$ represents the largest integer that is smaller than or equal to x . The above solution shows that the originally separated variables are recombined through the conformal transformation in the process of generating the spiral boundary.

The position vector of the logarithmic spiral is $\mathbf{r} = \rho e^{b\theta} \hat{e}_r$ in the polar coordinate system, where ρ is the distance from the spiral axis to the apical end of the spiral when the polar angle is zero; b is a parameter describing the spiral. The covering area of the spiral increases with b describing the compactness of the logarithmic spiral. On the outer wall, $\mathbf{r}_o = \rho_o e^{b\theta} \hat{e}_r$, the boundary condition of the impermeability of the cochlea wall requires that the normal component of the velocity should be zero;

$$U_{l,n}(\mathbf{r}_o, \theta) = \mathbf{U}_l(\mathbf{r}_o, \theta) \cdot \hat{e}_n = 0, \quad (17)$$

where \hat{e}_n is the unit vector normal to the spiral (see Appendix A). This condition provides relations between A_l and B_l as follows for $l = 1, 2, 3$;

$$B_1 = -bA_1, \quad (18)$$

$$B_2 = \frac{2b}{b^2 - 1} A_2, \quad (19)$$

$$B_3 = \frac{(3 - b^2)b}{3b^2 - 1} A_3. \quad (20)$$

And the velocity potentials for the three lowest modes are

$$\phi_1(r, \theta) = -A_1 \left(\theta + b \ln \frac{r}{\rho_o} \right), \quad (21)$$

$$\phi_2(r, \theta) = A_2 \left(\theta^2 - \ln^2 \frac{r}{\rho_o} + \frac{4b}{1 - b^2} \theta \ln \frac{r}{\rho_o} \right), \quad (22)$$

$$\begin{aligned} \phi_3(r, \theta) = & A_3 \left[\theta \left(3 \ln^2 \frac{r}{\rho_o} - \theta^2 \right) \right. \\ & \left. - \frac{(3 - b^2)b}{1 - 3b^2} \ln \frac{r}{\rho_o} \left(3\theta^2 - \ln^2 \frac{r}{\rho_o} \right) \right]. \end{aligned} \quad (23)$$

Since, we assumed that the RM is extremely flexible and, thus, behaves as a free boundary, the normal velocities of the inner side and the outer side are to be the same on the RM. We explicitly get the solution of the velocity potential of the outer part of the upper channel. According to Eq. (21), the normal velocity is always zero in the first mode. Consequently, this solution can be directly extended to the inner part of the cochlear duct. In this case, the fluid only has angular flux and the RM can be neglected in the mechanical model. However, for Eqs. (22) and (23), the fluid possesses normal flux. The normal velocity on the outer wall is zero but it is nonzero on the RM. Thus, it is expected that the RM critically influences fluid flow for the higher modes. In order to investigate this point more closely, we carried out a similar calculation on the inner part, from the inner wall to the RM. We find the normal velocities of the inner side and the outer side on the RM are virtually the same. Thus, we believe that when the stimulation is weak so that no excessive pressure can be build up at the RM and at the BM boundary, the assumption of the free boundary for the RM can provide at least a qualitative picture for the BM oscillation.

III. PRESSURE IN THE FLUID ACTING ON THE BM

The pressure of the fluid is governed by the Navier-Stokes (N-S) equation [17]. Viscosity of the lymph in the cochlear duct is usually negligible in the studies of hearing [7]. The inviscid N-S equation reads

$$\rho_{mass} \frac{DU}{Dt} = -\nabla P, \quad (24)$$

where ρ_{mass} is the density of the fluid; $D/Dt = \partial/\partial t + \mathbf{U} \cdot \nabla$; P is the pressure of the fluid. In the study of hearing, the disturbance of the fluid in the cochlea is usually small. Therefore, the pressure in the fluid can be obtained through the linearized N-S equation [17]

$$P = -\rho_{mass} \frac{\partial \Phi}{\partial t}. \quad (25)$$

The pressure in different modes can thus be obtained through the linearized N-S equation

$$P_l = -i\rho_{mass}\omega\phi_l(r, \theta) \cosh[\mu(\zeta - h)]T(t), \quad (26)$$

where we assume an input frequency ω . The fluid pressure right above and below the BM are P_{up} and P_{down} . When the upper channel is driven alone, the cochlear duct is expected to reduce the encountered large impedance through the lower channel. It has been shown that due to the symmetric structure of the upper and the lower channels and the connectivity of the helicotrema, we obtain an approximate relation $P_{\text{up}} \approx -P_{\text{down}}$ [12, 13]. Hence the net pressure in the mode l , which is the pressure difference between the upper and the lower channels acting on the BM, is

$$P_l^{\text{BM}}(r, \theta, t) = -2P_l(r, \theta, 0, t), \quad (27)$$

where P_l is the pressure in the upper duct in the mode l . We define a dimensionless tilt of pressure on the BM, which can be directly compared to the BM displacement tilt in Ref. [12], as

$$\Delta P_l^{\text{BM}} \equiv \frac{P_l^{\text{BM}}(r_o, \theta) - P_l^{\text{BM}}(r_c, \theta)}{P_l^{\text{BM}}(r_o, \theta_{\text{base}})}, \quad (28)$$

where $r_o(\theta)$ is the distance to the outer wall following the spiral arc, $\theta_{\text{base}} = 2K\pi$ with K being the number of the spiral turns, and $r_c(\theta)$ the distance to the center of the BM.

An arbitrary position vector on the BM can be expressed as $\mathbf{r} = \mathbf{r}_o + \sigma \hat{e}_n$, where σ is the normal distance from the outer wall to the position. Hence

$$\mathbf{r} = \left(\rho_o e^{b\theta} - \frac{\sigma}{\sqrt{b^2 + 1}} \right) \hat{e}_r + \frac{b\sigma}{\sqrt{b^2 + 1}} \hat{e}_\theta, \quad (29)$$

$$r = |\mathbf{r}| = r_o g \left(\frac{\sigma}{R_o} \right), \quad (30)$$

$$g \left(\frac{\sigma}{R_o} \right) = \sqrt{1 - \frac{2\sigma}{R_o} + (b^2 + 1) \left(\frac{\sigma}{R_o} \right)^2}, \quad (31)$$

where $R_o (= r_o \sqrt{b^2 + 1})$ is the radius of the curvature of the outer wall. Then, the dimensionless tilt of the pressure can be rewritten as

$$\Delta P_l^{\text{BM}} = \frac{\phi_l(r_o, \theta) - \phi_l(r_o g_c, \theta)}{\phi_l(r_o, \theta_{\text{base}})}, \quad (32)$$

where $g_c = g \left(\frac{\sigma_c}{R_o} \right)$ and σ_c is the half width of the BM. For the first and the second modes, we have

$$\Delta P_1^{\text{BM}} = -\frac{b}{2K\pi(b^2 + 1)} \ln g_c, \quad (33)$$

$$\Delta P_2^{\text{BM}} = \frac{1 - b^2}{(2K\pi)^2(b^2 + 1)^2} \left[\ln^2 g_c - \frac{2b(b^2 + 1)}{1 - b^2} \theta \ln g_c \right]. \quad (34)$$

IV. RESULTS AND DISCUSSIONS

Under the long-wave approximation, $\mu^2 \ll 1$ [12, 15], we have obtained the solutions of the three dimensional mechanical model of the spiral shaped cochlea. Now, we show that μ can be sufficiently small for any frequency as long as the stimulation is weak. As an example, we study the case of mode II ($l = 2$). Consider the velocity of the BM near $\zeta = 0$ at which the velocity of the BM reaches the maximum. The velocity of the BM is assumed to be the same as the velocity of the fluid on the BM. Therefore, the velocity of the BM can be represented by the velocity of the fluid as

$$U_{2,\zeta}(r, \theta, 0, t) = -\mu^2 h \phi(r, \theta). \quad (35)$$

In a weak stimulation, the velocity of the BM is very small, $\sim 10^{-5}$ m/s or less [18] in the passive system. Considering that the height of the cochlea is in the order of millimeter[19],

$$\mu^2 \phi(r, \theta) = \frac{-U_{2,\zeta}(r, \theta, 0)}{h} \sim 10^{-2}/\text{s}. \quad (36)$$

Hence, the small μ limit is consistent with not only the long-wave approximation but also the weak stimulation.

In the case of the lowest mode ($l = 1$) in which the flow has no normal flux, our results show that the dimensionless tilt of the pressure is a monotonic function of both the distance from the apex, θ , and the radius of the curvature, R_o . The maximum is at the apex, as shown in Fig 2. This is consistent with the previous theoretical result [12]. As shown in the Fig. 2b, the dimensionless tilt of the pressure is a scaling function of the radius of the curvature, $\Delta P_1^{\text{BM}} \sim R_o^{-1.08}$. This is in a close agreement to the result of the WKB-like approximation, $\Delta P_1^{\text{BM}} \sim R_o^{-1}$ [12]. In this mode, the solution can be directly extended from the outer part to the inner part. According to Eqs. (21) and (26), the pressure difference on the BM is also a monotonic function from the inner wall to the outer wall. In addition to this lowest mode, we find that there exist higher modes which show more complex behaviors. For example, in the second ($l = 2$) and the third modes ($l = 3$), the positions of the maximum of the tilt are determined by the compactness of the cochlea (described by b) and the reduced width of the cochlea (σ_c/ρ_o) as shown in Figs. 3-5. In these two cases, the solutions of the outer part cannot be directly extended to the inner part and the role of the RM may not be neglected. Our calculation reveals that except in the lowest mode, the distribution of

the resultant pressure acting on the BM is not only determined by the curvature of the cochlea but also influenced by the width of the cochlear duct (Fig. 4), which again implies the importance of the RM geometry in a more quantitative calculation. The amplitude of the tilt of the first responsive mode is larger than the tilt of the second and the third responsive modes in the apical region (Fig. 6).

The resultant pressure gradient in the radial direction induces the vibration of the hair cells on the BM. The pattern of the pressure tilt along the longitudinal length of the BM is therefore important for understanding the hearing mechanism. Previous work with the WKB-like approximation has shown that the curvature influences the tilt monotonically [12]. However, our results reveal that the influence of the shape can be more complex than that obtained by Manoussaki *et al.* [12].

The general solution of the pressure distribution in the fluid will be a linear superposition of various modes. To show the diversity of the pressure tilt along the BM, we now consider, for simplicity, only three lowest $\Phi_{sup} = (\alpha_1\Phi_1 + \alpha_2\Phi_2 + \alpha_3\Phi_3)/(\alpha_1 + \alpha_2 + \alpha_3)$, where α_1 , α_2 and α_3 are any real constants. In order to determine the relation between different A_i , we assume that the pressure at the basal end is same to the input pressure when each individual mode is allowed to exist alone. Since the coefficients appearing in the linear combination for a real oscillation cannot be determined a priori, thus, we assume two simple ratios of $\alpha_1 : \alpha_2 : \alpha_3 = 1 : 2 : 1$ and $\alpha_1 : \alpha_2 : \alpha_3 = 2 : 2 : 1$ and plot the tilt of the pressure of these two examples as superpositions of the modes in Fig. 7. The result shows that the maximum may not occur at the apex, but at a position not far from the apex. We believe that the exact maximum position is determined by the spiral and duct geometry of the cochlea and the detailed nature of the pressure wave. This result clearly indicates that the spiral curvature plays a decisive role in the wave energy redistribution in the cochlea as reported in the earlier calculation, although the detailed nature of the maximum position may be different from the WKB-like approximation [12]. Here, we note that we have assumed that the channels are fully filled with the fluid. If the channels are partially filled, the formulae and the results will be totally different.

V. CONCLUSION

In a long-wave approximation, the flow field of the three dimensional fluid is obtained analytically for the spiral shaped cochlear model. Pressure of the fluid is then calculated through the N-S equation. Result shows that the pressure acting on the BM is not uniform along the spanwise direction of the BM. Furthermore, the patterns of the pressure tilts along the longitudinal length of the BM are different for different modes. In general, the real pressure distribution is expected to be a linear superposition of various modes, although the simplest one may be dominant or at least substantial. Contributions from the higher modes are expected to push the pressure tilt maximum towards the basal end from the apex to a position which is determined by the curvature and the duct geometry. In conclusion, we have shown that the curvature of the cochlea plays a decisive role in hearing in addition to providing a compact storage.

Acknowledgments

This work was supported by the Korea Science and Engineering Foundation (KOSEF) grant funded by the Korea government (MOST) (R01-2006-000-10083-0).

APPENDIX A: UNIT VECTORS OF LOGARITHMIC SPIRAL

Let the position vector of the curve is \mathbf{r} . The unit tangent and normal vectors, as shown in Fig. 8, are respectively

$$\hat{e}_t = \frac{d\mathbf{r}}{d\theta} \bigg/ \left| \frac{d\mathbf{r}}{d\theta} \right|, \hat{e}_n = \frac{d\hat{e}_t}{d\theta}. \quad (\text{A1})$$

In the polar coordinate system, the position vector of the logarithmic spiral is

$$\mathbf{r} = \rho e^{b\theta} \hat{e}_r, \quad (\text{A2})$$

where \hat{e}_r is the unit vector in the r direction in the polar coordinate system. Consequently,

$$\hat{e}_t = \frac{1}{\sqrt{b^2 + 1}} (b\hat{e}_r + \hat{e}_\theta), \quad (\text{A3})$$

$$\hat{e}_n = \frac{1}{\sqrt{b^2 + 1}} (-\hat{e}_r + b\hat{e}_\theta). \quad (\text{A4})$$

-
- [1] H. Flecher, *Rev. Mod. Phys.* **12**, 47 (1940).
- [2] L. Robles and M. A. Ruggero, *Physiol. Rev.* **81**, 1305 (2001).
- [3] H. L. Helmholtz, *On the Sensations of Tone as a Physiological Basis for the Theory of Music* (Dover Publications Inc., New York, 1954).
- [4] P. Dallos, A. N. Popper, and R. R. Fay, eds., *The Cochlea* (Springer, New York, 1996).
- [5] A. W. Gummer, ed., *Biophysics of the Cochlea* (World Scientific, Singapore, 2003).
- [6] R. A. Eatock, R. R. Fay, and A. N. Popper, eds., *Vertebrate Hair Cells* (Springer, New York, 2006).
- [7] A. J. Hudspeth, *Curr. Opin. Neurobio.* **7**, 480 (1997).
- [8] G. von Békésy, *Experiments in Hearing* (McGraw-Hill Book Co., New Yourk, 1960).
- [9] M. A. Viergever, *J. Acoust. Soc. Am.* **64**, 1048 (1978).
- [10] C. H. Loh, *J. Acoust. Soc. Am.* **74**, 95 (1983).
- [11] C. R. Steele and J. G. Zais, *J. Acoust. Soc. Am.* **77**, 1849 (1985).
- [12] D. Manoussaki, E. K. Dimitriadis, and R. S. Chadwick, *Phys. Rev. Lett* **96**, 088701 (2006).
- [13] A. Kern, Ph.D. thesis, Swiss Federal Institute of Technology (ETH), Zürich (2003).
- [14] M. Homer, A. Champneys, G. Hunt, and N. Cooper, *J. Acoust. Soc. Am* **116**, 1025 (2004).
- [15] J. Lighthill, *J. Fluid Mech.* **106**, 149 (1981).
- [16] K. F. Riley, M. P. Hobson, and S. J. Bence, *Mathematical Methods for Physics and Engineering* (Cambridge University Press, Cambridge, 2006), 3rd ed.
- [17] J. Lighthill, *Waves in Fluid* (Cambridge University press, Cambridge, 2005).
- [18] M. A. Ruggero, S. S. Narayan, A. N. Temchin, and A. Recio, *Proc. Natl. Acad. Sci. USA* **97**, 11744 (2000).
- [19] C. R. Steele and L. A. Taber, *J. Acoust. Soc. Am.* **65**, 1007 (1979).

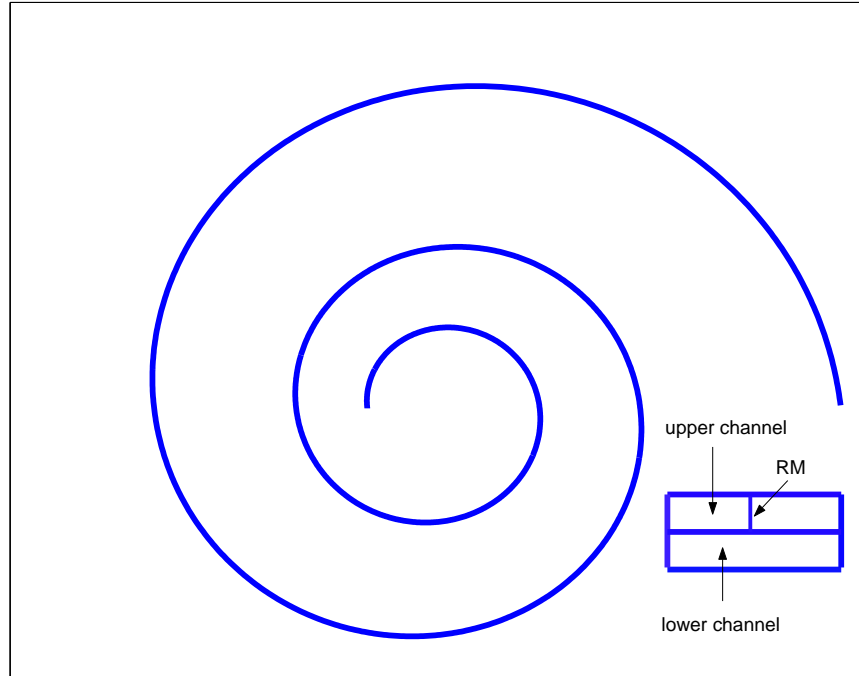


FIG. 1: Sketch of the shape of the cochlea in the present model. The top view of the cochlea is modeled as a logarithmic spiral; the cross section of the cochlea is approximated as a rectangle with constant width and height along the entire length of the cochlea. The duct of the cochlea is divided by the BM into two channels.

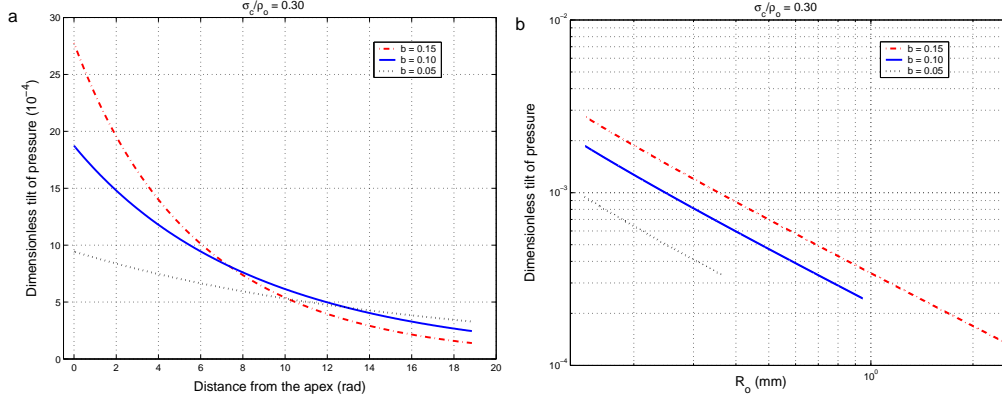


FIG. 2: (color online). The pressure tilt in the mode I ($l = 1$). The maximum always appears at the apical end. For σ_c/ρ_o , we use 0.3. (a): The tilt is plotted as a function of the distance from the apex. (b): The dimensionless pressure tilt is a scaling function of the radius of the curvature, R_o . The slope of the straight lines is about 1.08. Therefore, it reveals that, in this mode, our result is consistent with the previous theoretical result [12].

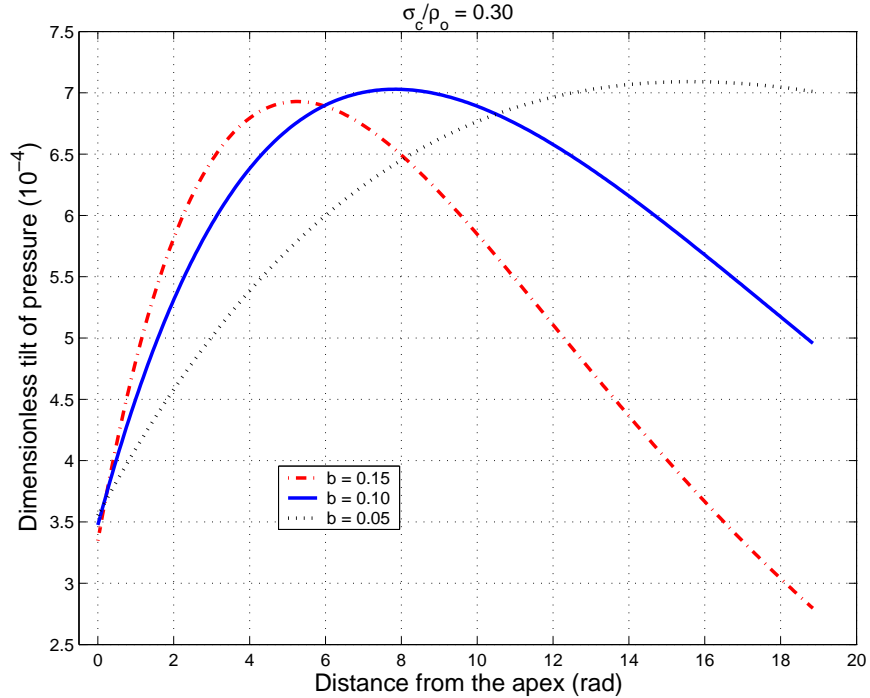


FIG. 3: (color online). In the mode II ($l = 2$), the tilt of the resultant pressure acting on the BM. It reaches a maximum and decreases along the longitudinal length of the cochlea. The position of the maximum depends on σ_c/ρ_o and b .

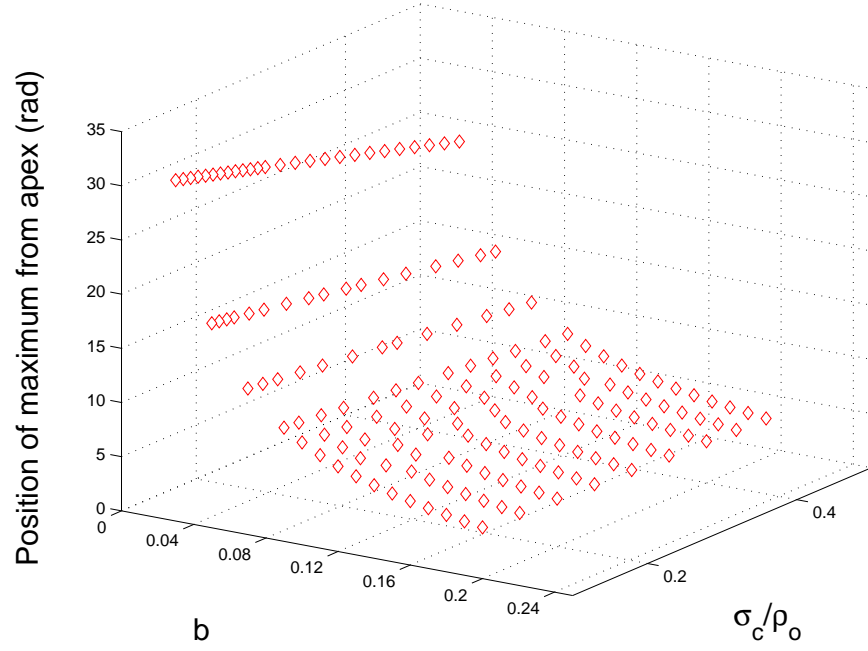


FIG. 4: In the mode II, the maximum of the tilt appears at a position along the longitudinal length of the cochlea. It is determined by both the compactness and the width of the cochlea.

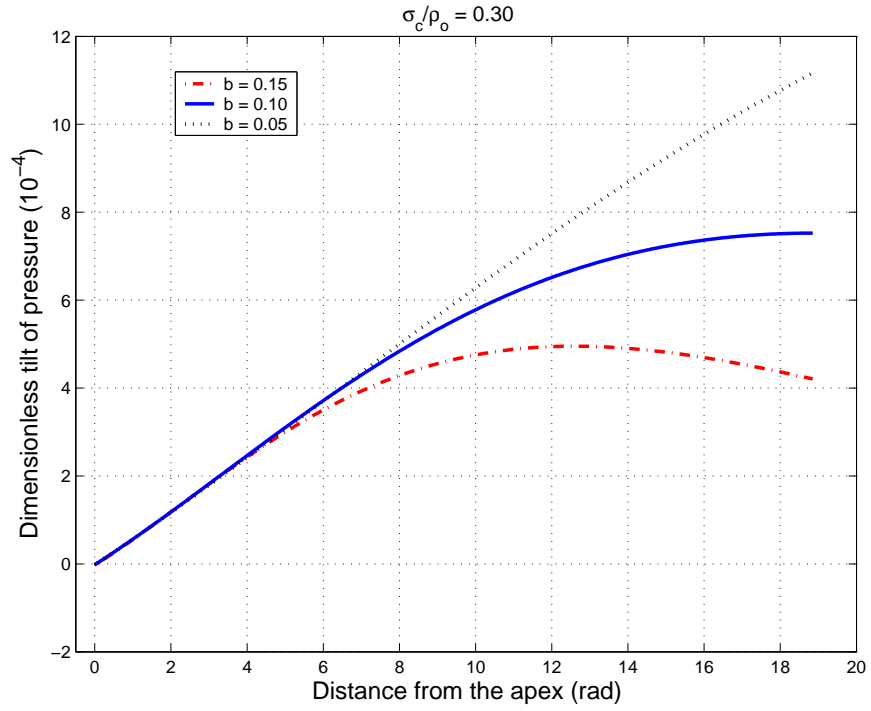


FIG. 5: (color online). The tilt of the pressure in the mode III ($l = 3$). The curves are calculated at $\sigma_c/\rho_o = 0.3$. The maximum of the tilt appears at a position determined by the geometry of the cochlea.

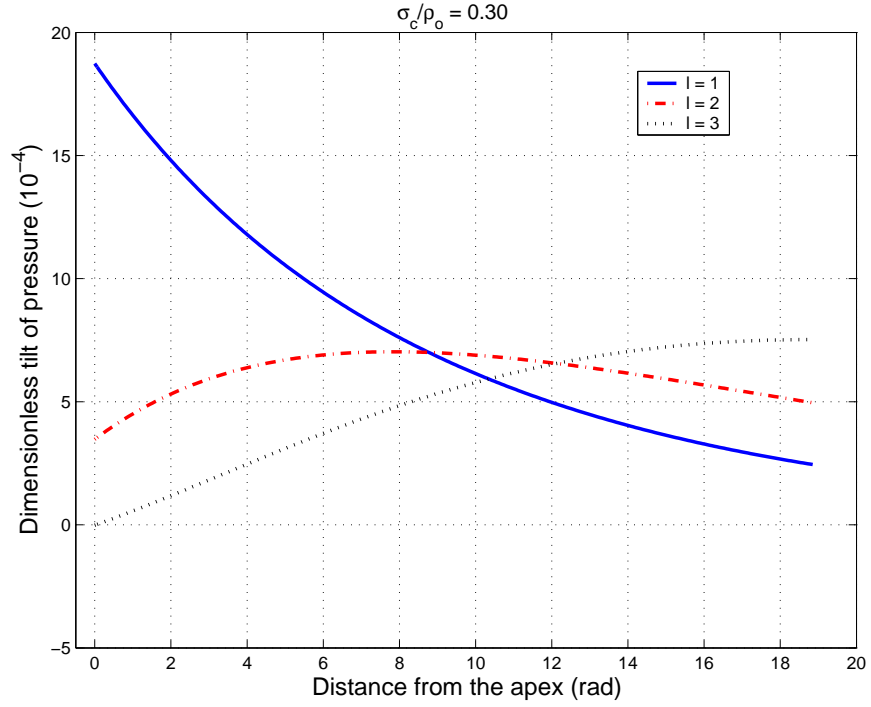


FIG. 6: (color online). A comparison of the tilt of the resultant pressure for the first three modes. $b = 0.10$, $K = 3$ and $\sigma_c/\rho_o = 0.3$. In the apical region, the tilt of the first responsive mode is larger than the tilt of the second mode; The tilt of the second responsive mode is larger than the tilt of the third mode.

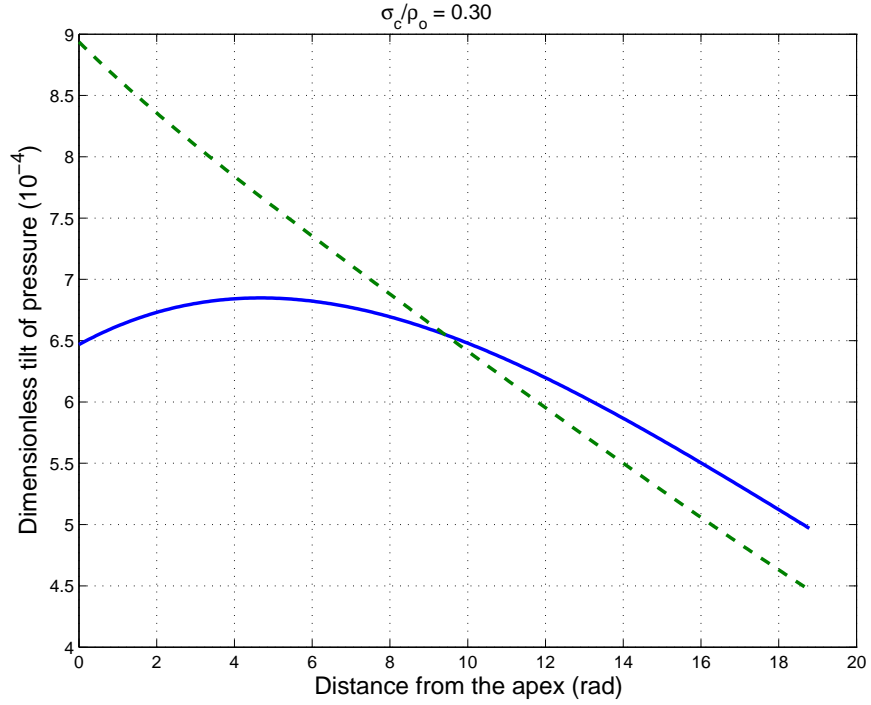


FIG. 7: (color online). Linear superpositions of the first three modes. The maximum of the tilt is located at a position determined by the coefficients of the superposed modes and the geometry of the cochlea. $b = 0.10$, $K = 3$ and $\sigma_c/\rho_o = 0.30$. Solid line corresponds to $\alpha_1 : \alpha_2 : \alpha_3 = 1 : 2 : 1$. Dash line corresponds to $\alpha_1 : \alpha_2 : \alpha_3 = 2 : 2 : 1$.

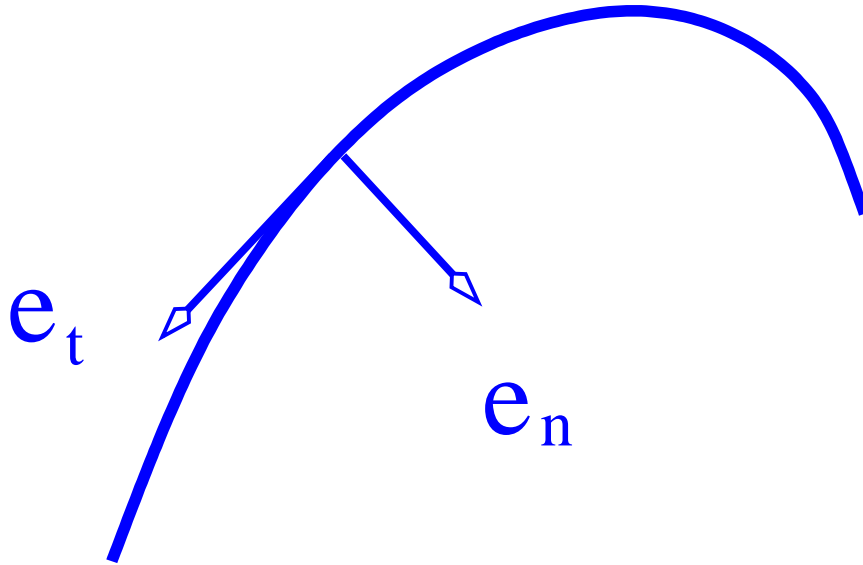


FIG. 8: The unit tangent vector, \hat{e}_t , and the unit normal vector, \hat{e}_n , of a logarithmic spiral.